NEOPLASIA
www.neoplasia.com
Volume 21 Number 11 November 2019 pp. 1091–1101

Fibrin Deposit on the Peritoneal Surface Serves as a Niche for Cancer Expansion in Carcinomatosis Patients

Shah Shahid*,[1]; Aldybiat Iman*; Ullah Matti*; Kaci Rachid; Alassaf Assaf*; Clarisse Eveno*; Pocard Marc*; Mirshahi Massoud*,*

*CAP-Paris Tech., INSERM U1275, Hpital Lariboisire, 2, rue Ambroise-Par, 75010, Paris, France Central Department of Anatomy and Pathological Cytology, Hospital Lariboisire, 75010, Paris, France Address all correspondence to: M. Mirshahi MD, PhD, University of Sorbonne Paris Cit -Paris 7, Lariboisire Hospital, INSERM U1275, 75010, 75010, Paris, France.

Abstract

Peritoneal metastasis (PM) is a very serious complication of gastrointestinal and gynecological malignancies which is poorly documented. Modified mesothelial cell layer and their microenvironments can favor fibrin deposition for cancer cell adhesion. Scanning and transmission electron microscopy of peritoneal surface and cancer cell clusters from cancer patients was done. Ascites and its impact on mesothelial cells were assessed by cytokine array. Neprilysin, matrix metalloprotease, epithelial mesenchymal transition (EMT) related molecules (Ecadherin, Snail, Slug, Twist, Vimentin and Fibronectin), tissues factor (TF), endothelial protein C receptors (EPCR) were quantified by qPCR. Fibrin in the simples were stained using anti fibrin F1E1 antibody. Migration ability was assessed by scratch assay. Cell viability and neprilysin activity were analyzed by bioluminescence. Cancer cellsfibrin interaction was investigated by scanning electron microscopy (SEM) and microcinematography (MCG). Mesothelial cells change their morphology after incubation with carcinomatosis peritoneal fluids *in vitro*. EMT associated with upregulation of neprilysin, matrix metalloproteinase2, tissue factor and cytokines secretions such as interleukin6, and 8, hepatocyte growth factor and granulocyte chemotactic protein2 mRNA and protein were observed. EPCR expression as a natural anticoagulant was decreased. In parallel, carcinomatosis cell clusters extracted from peritoneal fluids were found to be associated with fibrin. Kinetic analysis of cancer cellfibrin interaction *in vitro* studied by MCG showed that fiber filaments generated from clots inhibited cancer cell adhesion on fibrin clots. These results indicated that fibrin deposit on the peritoneal surface serve as niches for cancer expansion in carcinomatosis patients.

Neoplastic (2019) 21, 1091–1101

Introduction

The tumor sheds cells into the peritoneal cavity which implant on a membrane (mesothelium) and cover the peritoneal surfaces [1]. Complex bidirectional interactions between metastatic cancer cells and peritoneal environment seem to be crucial for colonization on the peritoneal wall. The peritoneal environment is receptive to cancer seeding [2]. A common feature of the peritoneal environment is the mesothelial lining to which cancer cells must bind successively [3,4] and penetrate [5] to adhere to the underlying tissues. Recent *in vitro* studies suggest that this penetration step may take place a few hours after the fixation of metastatic cancer cells [6]. These cells can then adhere to the surface of peritoneal organ and seed new tumors, favored by the chemokines and growth factors within the peritoneal fluid [7].

Epithelial mesenchymal transition (EMT) in mesothelial cells plays an important role in the processes of peritoneal membrane fixation and invasion [8]. Electron micrographs of tumor associated with excised human peritoneum revealed that mesothelial cells are not present directly beneath the tumor mass, suggesting mesothelial clearance of the area below the tumor mass [9]. To the best of our knowledge, the cellular and molecular mechanisms of mesothelial clearance are still unknown.

Mesothelial cells are flat cells that produce a small amount of lubricating fluid inside the abdomen with a dynamic cellular membrane and provide a slippery, nonadhesive and protective surface [10]. Mesothelial monolayer covers the peritoneal cavity and its associated organs are the major site for development of secondary tumor [11]. Extracellular matrix and adhesion molecules constitute a great part of the tumor microenvironment. Several hypotheses such as adhesion of cancer cell *via* mesothelial cells or mesothelial basement membranes have been proposed [8,12] and the role of VCAM1 [13], α31 integrin [14] as well as MMP [15], TGF [16], EGF [17], HGF [18] and VEGFA and C were investigated [19]. In cancer treatment, a complicated postoperative healing scar corresponds to an increase in the incidence of tumor expansion [20].

[1] Present address: Department of Pharmacy Practice, Faculty of Pharmaceutical Sciences, Government College University, Faisalabad, Pakistan.
e-mail address: massoud.mirshahi@inserm.fr (M. Massoud)

Received 18 May 2019; received in revised form 17 August 2019; accepted 20 August 2019;

However, the impact of wound healing processes on the peritoneal microenvironment, such as fibrin deposition, as well as the behavior of mesothelial cells in cancer associated pathologies has not been reported. Here we studied the expression of procoagulant and proteolytic enzymes in the tumor microenvironment to modify peritoneal surfaces during carcinomatosis expansion.

Materials and Methods

Cell Lines

Normal adult human mesothelial cells were purchased from Zen Bio, Inc. (Research Triangle Park, North Carolina, USA) and CT26 (colon cancer) from American Type Culture Collection (ATCC, Manassas, VA). The two cells (mesothelial cells and CT26) were maintained respectively in mesothelial cell growth medium (ZenBio, Inc.) and DMEM (Gibco, Saint Aubin, France). The cellular environment was maintained at 50 ml/L CO_2 and 37°C.

Patients

Peritoneal membranes (ovarian cancer patient) and six freshly isolated ascites fluids (ovarian n = 2, gastric n = 2 and colic n = 2 cancer patients) were obtained from the General and Digestive Tract Surgery Department at Lariboisire Hospital in Paris (France). Informed consent was obtained from each patient prior to surgery. The cells (210^5/200 l) of peritoneal liquid (n = 6) were sedimented by a short spin at 3000 rpm for 10 min at 20° C. Ascites fluids obtained from cancer patient (n = 6) were used after centrifugation at 1200 rpm for 5 min and preserved at 80°C.

Fluorometric assays

A substratebased activity assay kit (AnaspecSensoLyte, Belgium) that determines the activity of neprilysin was used according to the manufacturer's instructions. Briefly, equal amounts of cell lysates of mesothelial cells grown in medium with or without 25% ascites for 6 days were used. Aliquots from each sample were incubated in the presence of the neprilysin substrate solutions for 60 min. The fluorescent product was measured in a spectrophotofluorometer (GloMaxMulti Detection System, France) with excitation at 490 nm and emission at 520 nm.

Immunohistochemistry

Samples of invasive and noninvasive peritoneum and tumor tissue were obtained from patients and used for this study. For anatomopathological analysis, the samples were dissected, fixed in 4% paraformaldehyde (PFA) and embedded in paraffin. The slides (4 micron) were prepared and stained with hemateineosinsafran according to conventional methods in the anatomopathological laboratories. Similarly, slides were also prepared using cytospin for ovarian cancer ascites cells. In parallel, several slides were stained with peroxidasecoupled antibodies using a Benchmark Ultra apparatus (Roche Ventana, Tucson, AZ, USA) according to the protocol of their manufacturers. The antibodies used for immunohistochemistry were: anti Ecadherin (1/50), Ki67 (1/50), CD31 (1/20), D2–40 (undiluted) from Glostrup USA and cytokeratin (1/50), WT1 (1/50) from Carpinteria, California, USA, F1E1 (anti fibrin antibody 1/50) from our laboratory [21]. The images were taken by Leitz microscope (Diaplan) with a Nikon Cool pix 995 apparatus (Japan).

Scanning Electron Microscopy

The peritoneal membranes were fixed using 4% PFA for 24 h and washed with PBS buffer (1) three times each for 5 min. Then 2% glutaraldehyde was added to the membrane for 20 min and washed with PBS buffer (1) three times each for 5 min. After a final wash with distilled water, the samples were dehydrated in increasing concentrations of ethanol. The samples were gold plated by sputtering after drying. These were observed with a S260 CAMBRIDGE scanning electron equipped with a LaB6 filament operating at 15 kV and the images were captured using the Orion software from (NCH Software).

Transmission Electron Microscopy

The primary ovarian cancer cells with fibrosis were detected using transmission electron microscopy. Briefly, the primary cells, after their ascites recovery, were cultured in DMEM medium. Cells (100 million) were harvested, pelleted and then fixed in 4% PFA for 15 min. The samples were then rinsed with PBS (1). Ultrafine sections (50 to 70 nm) were cut using a Leica RM2235 ultramicrotome (Leica Microsystems GmbH, Wetzlar, Germany) and observed under a transmission electron microscope (Hitachi H800; Hitachi, Tokyo, Japan).

Microcinematography (MCG)

To document the kinetics of CT26 cells in the presence of fibrin, timelapse MCG was done. Briefly, 100 l of human plasma with 2 U of thrombin and 30 l of 0.025 M $CaCl_2$ (Diagnostic STAGO, Parsippany, USA) were prepared in a 6well plate. After 30–45 min, CT26 cells (5 10^5/well) were seeded on thrombin clot in medium. The plate was placed in the stagetop environmental chamber. A specific area was focused where there was a maximum chance of observing the interaction between the cancer cells and thrombin clot. MCG was performed to acquire images after every 2 min for 24 h to 48 h in order to study the migration behavior of CT26 in a controlled temperature room of 37 °C in a humidified atmosphere (>80%) containing 5% CO_2 using an EVOS FL Auto Imaging System (Life Technologies, Waltham, MA, USA). The distance traveled by the cancer cells was calculated in micrometer while the average speed in micrometer/min was obtained by dividing the total distance traveled by the time required to cover this distance.

Wound Healing Assay

The mesothelial cells were cultured (80% confluence) in a 12well plate with or without 25% ovarian ascites for 6 h, 12 h, 24 h or 36 h. The migration ability of mesothelial cells was evaluated by means of a scratch assay. A denuded area was generated on quiescent cell monolayers of mesothelial cells by scratching with a sterile pipette tip. The monolayer was washed twice with PBS (1) and then incubated for 24 h in medium having no FBS. The cells were photographed at different time. The width of the scratch was measured at three different places in the photograph to obtain an average value after different time intervals. The wound closure rate (m/h) was calculated as the slope of the line obtained after plotting a graph; width *versus* time interval.

RNA isolation, RT and real-time PCR

Total RNA in the cells was extracted using the Qiagen RNeasy Mini Kit (Qiagen, Germany) according to the manufacturer's instruction. The RNA samples were transcribed into cDNA in a 20 l volume, using the QuantiTect reverse transcription kit (Qiagen).The thermal cycle included the following realtime PCR conditions: 95°C for 5 min, followed

by 40 cycles (denaturation for 15 sec at 95°C, annealing for 20 sec at 60° C) and extension for 20sec at 72°C). The primers sequences and the size of the PCR product for the target and reference gene are listed in supplementary results table S1. The expression levels of mRNA of different markers were detected by realtime PCR with actin as internal reference, using Mesa Blue qPCR Master Mix Plus for SYBR assay (Eurogentec) on the Master cycler Realplex2 (Eppendorf).The PCR products of cell lines and tissue samples, after realtime PCR, were electrophoresed by EGel Precast Agarose Electrophoresis System (Thermo Fisher Scientific Inc., Waltham, USA).

Cytokine Array

We examined the supernatant of mesothelial cells cultured in 25% ovarian ascites using a protein cytokine array (RayBio Human Cytokine Antibody, Norcross, GA, USA). This technique is based on the principle of sandwich immunoassay. It comprises essentially of screening, in duplicate, 174 different membranecoupled anticytokines along with appropriate controls. Mesothelial cells (0.2510^6 cells/ml) were incubated in RPMI medium having no fetal bovine serum with or without 25% ovarian ascites at 37°C in a humidified atmosphere of 5% CO_2 for 24 h. Supernatants containing cytokines were retrieved and processed according to the manufacturer's protocol. The presence of antibody coupled proteins was revealed by applying ECL (enhanced chemiluminescence) to the membranes, according to the manufacturer's recommendations. The membranes were then exposed to photosensitive film (Kodak, XOMAT, AR, USA).

The intensity of chemiluminescence captured on the photosensitive film was measured and recorded. After subtracting the background noise, the results were expressed as a ratio of the chemiluminescence intensity of experimental *versus* control spots.

Cell Viability Assay

Cell viability was assayed by Real TimeGlo MT cell viability assay. Briefly, cells (5 10^2/well) were seeded in 96well plates, following 24 h later by treatment with 25% gastric, colic or ovarian ascites for 48 h. Bioluminescence was measured with spectrofluorometer SAFAS Xenius XC. Cell viability was expressed as the percent absorbance of the ascitestreated cells relative to that of the controlled cells. Each condition was done in triplicate. The experiment is representative of three independent lots.

Results

Change in the Morphology of Mesothelial Cell Layer and Fibrin Deposition on the Peritoneal Wall

As presented in Figure 1, mesothelial cell layer in the noninvasive peritoneal region forms a continuous line when the cells of the peritoneal sample were stained with Ecadherin (Figure 1*A*). In invasive regions, the mesothelial cell layer is perturbed in certain areas of the peritoneal membrane and forms a discontinuous line under the same conditions (Figure 1*B*). Figure 1*C* presents the scanning electron microscopy (SEM) analysis of the noncarcinomatous peritoneal membrane. The mesothelial cells (arrow) with the plicate layer show the normal cell–cell interaction forming a homogenous layer. Figure 1*D* shows a SEM analysis of the invasive peritoneum in which mesothelial cell detachment of the submesothelial cell layer was noticed.

Fibrin deposits on the mesothelial cell layer of peritoneal metastasis were analyzed by classical anatomopathological studies as well as by immunohistochemistry. As presented in Figure 1*E*, noninvasive peritoneal wall in patients with carcinomatosis were analyzed by photonic microscopy. As shown in Figure 1*F*, several regions with fibrin deposition were observed. In some regions, cancer nodules (red arrow) were observed on the fibrin net (Figure 1*G*). The presence of fibrin on the peritoneal wall may be a consequence of procoagulant activity *via* mesothelial tissue factor as well as submesothelial collagen in these regions and confirmed using human antifibrin monoclonal antibodies. Figure 1*H* shows the noninvasive region of the peritoneal surface, where the mesothelial cells were stained with anticytokeratin antibody (white arrow). Figure 1, *I* and *J* present the peritoneal walls from two patients respectively in that the fibrin deposition detected in the intermesothelial cells space (Figure 1*I*) or on the entire surface (red arrows).

The SEM analysis of the noninvasive peritoneum shows an unchanged and uninterrupted surface covered with mesothelial cells (Figure 1*K*). The surface of the mesothelial layer was intact and the cells were naturally arranged. On the other hand, in the invasive regions, the mesothelial cells were deformed and fiber nets were deposited in the intermesothelial cell space (Figure 1, *L* and *M*). The interaction of cancer cells with fibrin deposition is presented in Figure 1*N*.

Fibrin Deposition on the Peritoneal Wall Associated With Angiogenesis and Lymphangiogenesis

Figure 2, *A–D* presents the noninvasive region of the peritoneum. The mesothelial cells were stained with anti–cytokeratin antibody that reacts only with the epithelial cells (Figure 2*A*). The blood vessels were stained with an anti CD31 antibody. CD31 was present on the platelets, monocytes, granulocytes, B lymphocytes and intracellular endothelial junction (Figure 2*B*). The lymphatic wall was stained with anti D2–40 antibody (Figure 2*C*). This antibody also reacts with mesothelial cells. Figure 2*D* presents all the cells that are in division cycle stained with the Ki67 antibody.

In invasive regions (positive for Ki67), the presence of fibrin deposition was associated with high expression of CD31 (Figure 2*E*) and D2–40 (Figure 2*F*). As presented in Figure 2*G*, the proliferative cells are present in fibrin deposits as well as peritoneal tissues. The number of blood vessels and lymphatic vessels in the noninvasive and invasive regions of the peritoneum is presented in Figure 2*H*. Interestingly, the blood vessels in fibrin deposition area contain more mononuclear cells than other areas reflecting earlier inflammatory events.

Figure. 1. Mesothelial cell layer in the non-invasive and invasive peritoneal region and cancer cell clusters in ascites. Invasive and non-invasive peritoneal region by immunohistochemistry of E-cadherin (A and B) and scanning electron microscopy (C and D). Mesothelial cell (MC) shown by black arrow. Eosin hematoxylin and immunohistochemical detection of cytokeratin (mesothelial layer shown by the white arrow) on the non-invasive peritoneum were presented respectively in (E and H). Similarly, the fibrin deposition and the cancer nodule on the invasive peritoneal surface presented with yellow and red arrow respectively (F, G and I, J). Scanning electron microscopy analysis of non-invasive (K) and invasive peritoneum (L, M and N) demonstrated the intermesothelial surface (black arrow). The presence of fibrin network identified on the inter-mesothelial (basement membrane) space (yellow arrow, M and N) and the cancer cell interaction with fibrin network (N).

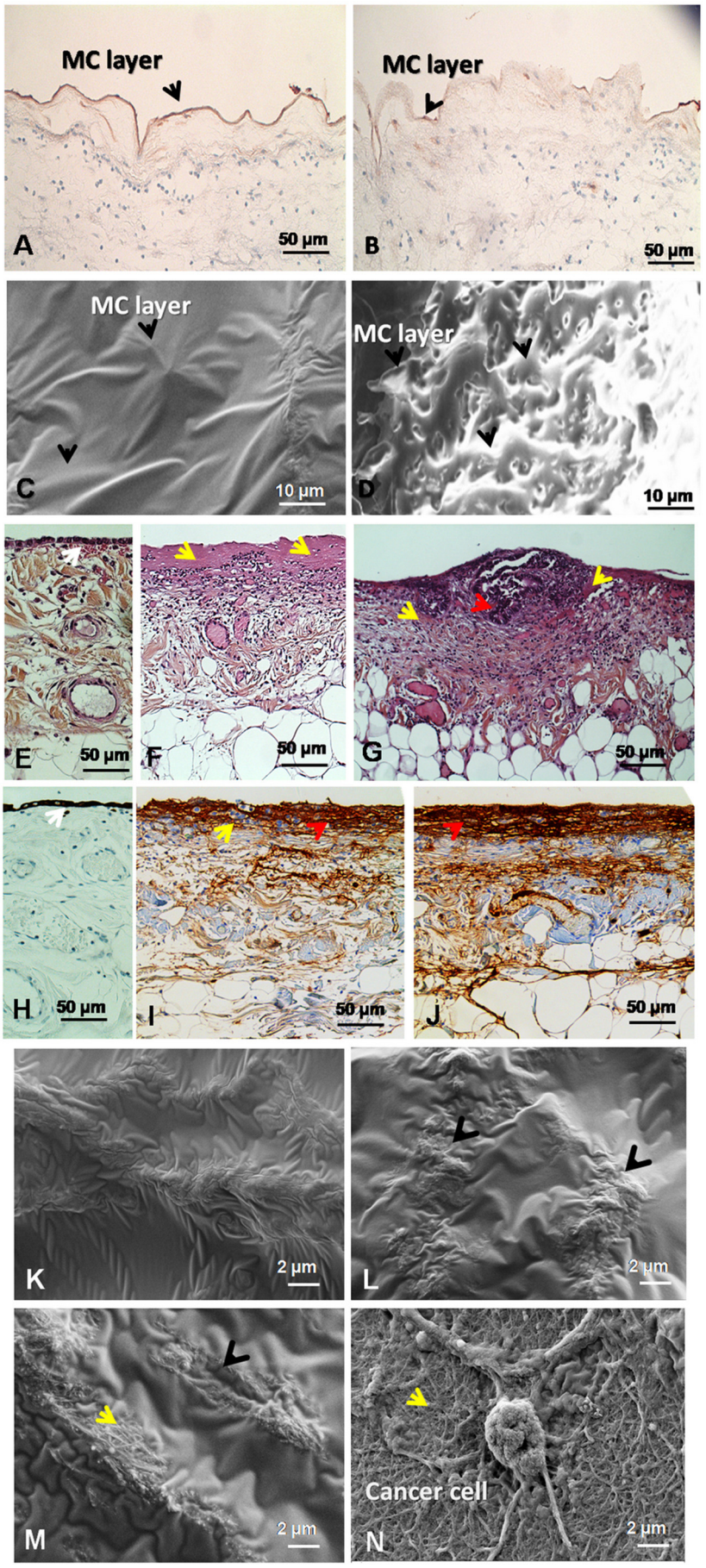
MC layer
A
50 μm
MC layer
B
50 μm
MC layer
C
10 μm
MC layer
D
10 μm
E
50 μm
F
50 μm
G
50 μm
H
50 μm
I
50 μm
J
50 μm
K
2 μm
L
2 μm
M
2 μm
Cancer cell
N
2 μm

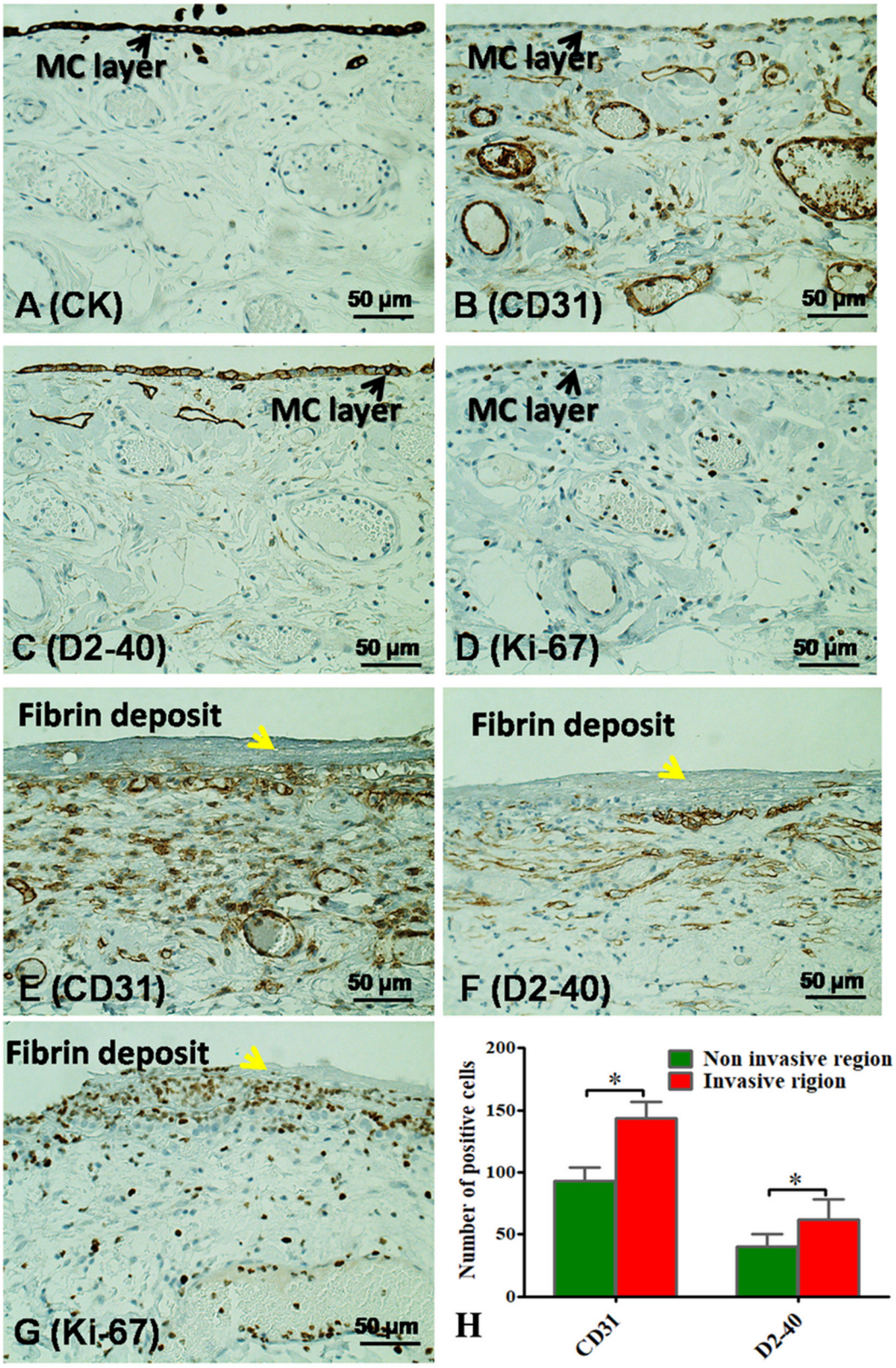

Figure 2. Immunohistochemistry of non-invasive and invasive peritoneal region. Immunohistochemical detection of cytokeratin (CK) on the mesothelial cell (MC) layer, CD31 (endothelial cells of blood vessels), D2–40 (endothelial cells of lymphatic vessels that cross react with mesothelial cells) and Ki-67 (proliferative marker) in non-invasive region (A, B, C and D) and of CD31, D2–40 and Ki-67 in invasive region (E, F and G) of peritoneum were presented. The fibrin deposition identified with yellow arrows in E, F and G. Statistical data for the number of CD31 and D2–40 stained cells in non-invasive and invasive regions is presented (H). Data were obtained from each of 20 invasive and non-invasive areas of a single preparation. $^{*}P < .05$.

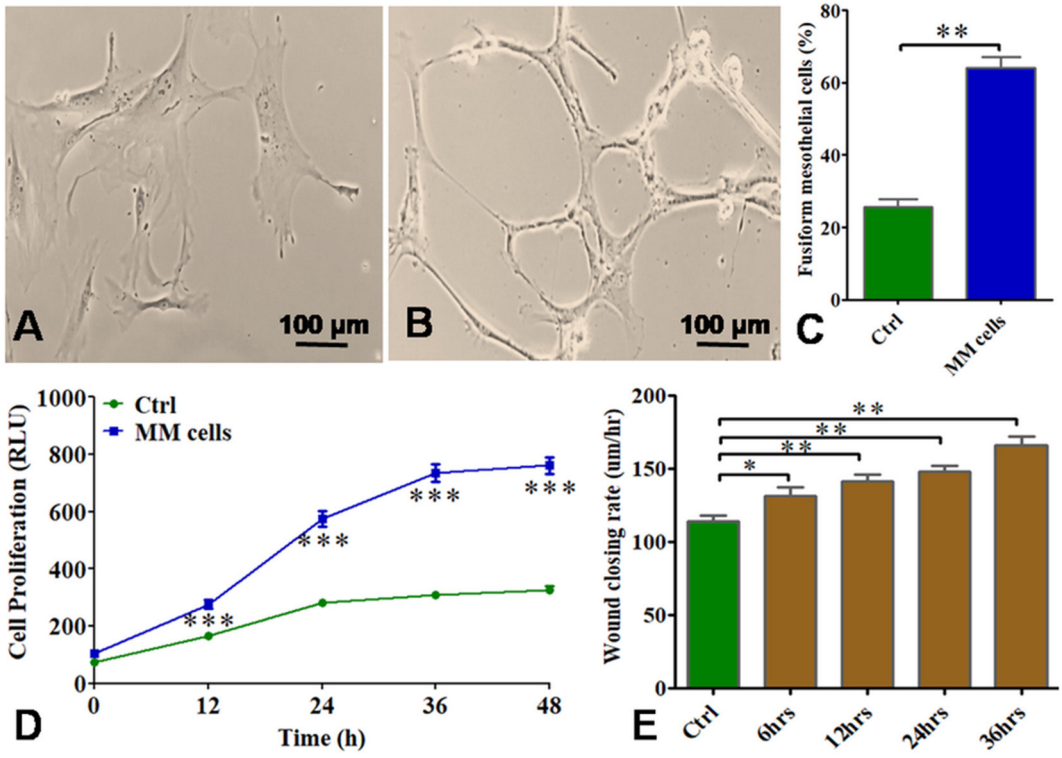

Figure 3. Ovarian ascites induces modification in cell shape, proliferation and migration of mesothelial cells. Morphology of mesothelial cells before (A) and after (B) treatment with ovarian ascites. % age fusiform of mesothelial cells after treatment of 25% ovarian ascites (C). Modified mesothelial cells (MM cells) proliferate (D) and migrate (E) rapidly in the presence of 25% ovarian ascites. The results are expressed as mean SEM of six independent experiments. $^{*}P < .05$, $^{**}P < .01$, $^{***}P < .001$ compared with the control (Ctrl).

Peritoneal Fluid from Ovarian Carcinomatosis Modified Mesothelial Cell Behavior In Vitro

For the analysis of the impact of ovarian peritoneal fluid on mesothelial cells, we tested the effect of medium containing 25% ovarian ascites on cell shapes, cell proliferation and cell migration *in vitro*. When the mesothelial cells were incubated with ascites, they acquired a fusiform shape. Figure 3 presents the shape of the mesothelial cell shapes *in vitro* before (3A) and after (3B) incubation with ascites. The numerical results are presented in Figure 3*C* ($P = .01$). The presence of ascites in the culture medium increases significantly mesothelial cell proliferation ($P = .001$) and wound healing ($P = .01$) in a timedependent manner (Figure 3, *D–E*). These results are support the influence of ascites on the mesothelial cell layer as observed by microscopy.

Ovarian Ascites Contains Biologically Active Proteins and Alters the Secretion of Cytokine by Mesothelial Cells In Vitro

We tested several peritoneal fluids from ovarian carcinomatosis by cytokine array analysis. The cytokine profile was detected in two patients with ovarian cancer and is presented in supplementary results Figure S1. The results indicate the presence of several groups of cytokines in each ascites involved in cancer cell growth and progression, angiogenic and lymphangiogenic stimulation, mesothelial cell activation, immune cell activation/inhibition, cell adhesion, membrane permeabilization and procoagulant activity. When mesothelial cells were grown in a medium without serum and other biological additives (conditioned medium) followed by incubation with 25% ovarian ascites for 24 h *in vitro*, the profile of cytokines pattern was changed. Mesothelial cells secret a high amount of IL6, MCP1, GRO, ANG, OPG, IL8 and TIMP1 in conditioned medium. The presence of ovarian ascites in culture medium could modify and increase cytokines secretion from the mesothelial cells as presented in Figure 4*A*. Among upregulated proteins, the effect of IL6, IL8, HGF and GCP2 were tested separately on mesothelial cells in conditioned medium. The levels of mRNA folds for metalloprotease, procoagulant and proanticoagulant are presented in supplementary results table S2. These results indicate the upregulation of metalloprotease MMPs and neprilysin as well as tissue factor and fibronectin *via* an autocrine pathway (Figure 4, *B–E*).

Ovarian Ascites Induces EMT Markers and Regulates Proteolytic Enzymes and Procoagulant Factors in Mesothelial Cells

Mesothelial cells in the culture medium express basal amounts of EMT markers such as Snail, Slug, Vimentin, Fibronectin and Twist (Figure 5*A*). The basal amount of these markers as well as Ecadherin is presented in Figure 5*B* (green colors). When these cells were incubated in culture medium supplemented with 25% ovarian ascites, all EMT markers, except Ecadherin, were upregulated as presented in Figure 5*B*. These results indicate the narrow correlation between cell shape modification and epithelial mesenchymal transition.

The basal mRNA expression of several metalloproteases (neprilysin, MMP2 and MMP9), procoagulant factors (tissue factor TF) and antiprocoagulant factor (endothelial protein C receptor EPCR) as well as neprilysin activity of the mesothelial cells are presented in Figure 5, *D–F* (green colors). When these cells were incubated for 48 h in culture medium supplemented with 25% ovarian ascites, the expression of all markers, except EPCR, were upregulated. The results presented in Figure 5*D* demonstrate the upregulation of TF and down regulation of EPCR. These results support the global procoagulant activity of mesothelial cell

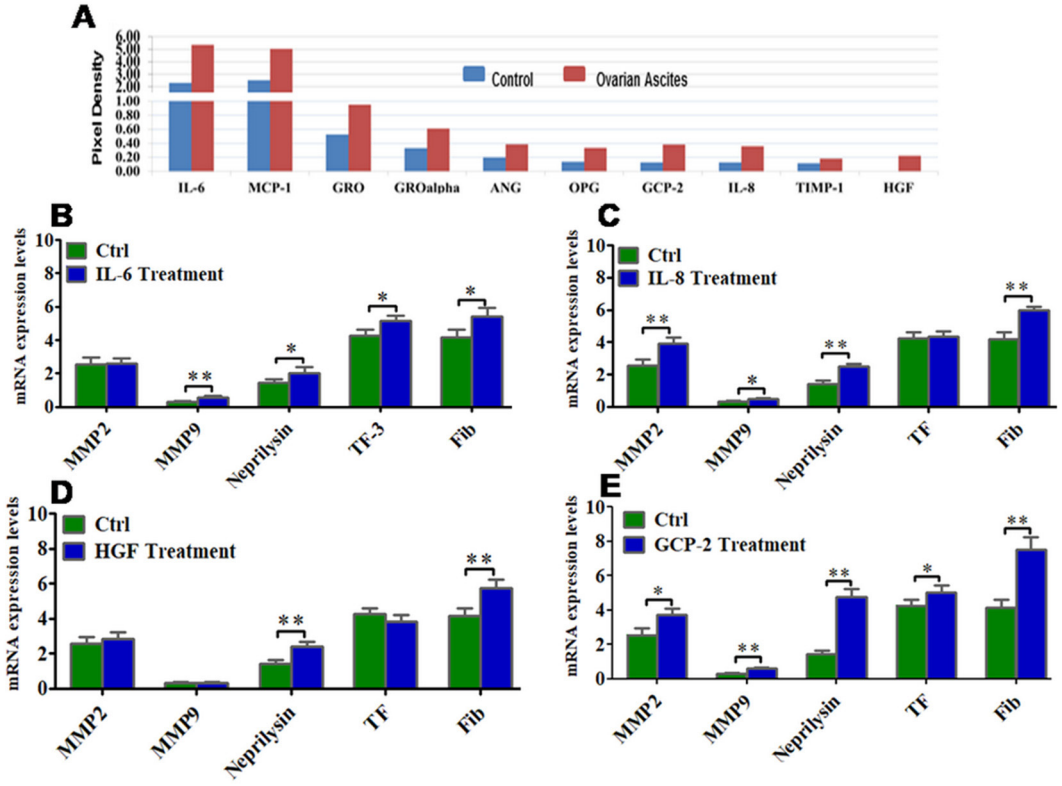

Figure 4. Relative expression of various cytokines and mRNA of metalloprotease, procoagulant and proanticoagulants in mesothelial cells after treatment with ovarian ascites. The histogram shows the relative expression of cytokines (IL-6, MCP-1, GRO, GRO-α, ANG, OPG, GCP-2, IL-8, TIMP-1, HGF) secreted from mesothelial cells in their supernatant after treatment with ovarian ascites (A). mRNA of metalloprotease (MMP-2, MMP-9 and Neprilysin) and procoagulant (TF) were found in mesothelial cells after treatment with exogenous cytokines IL-6 (B), IL-8 (C) and growth factors HGF (D), GCP-2 (E) by qPCR. The results are expressed as mean SEM of six independent experiments. *$P < .05$, **$P < .01$, compared with the control (Ctrl).

microenvironments. Among MMPs, the neprilysin, MMP2 and MMP9 were expressed higher shown in Figure 5*E*. Neprilysin activity was also found at a higher level presented in Figure 5*F*. Consequently, ascites–mesothelial cell interaction induces the expression of membrane bound enzyme neprilysin as well as MMP2. When mesothelial microenvironment is modified by ascitic fluid, the high expression of MMPs and neprilysin can be an inductor of mesothelial detachment from the peritoneal membrane. As presented in Figure 5, *G* and *H*, the carcinomatosis cell clusters contain the mesothelial cells stained with D2–40 and WT1 antibodies respectively.

Occurrence of Cancer Cell Cluster Associated with Fibrin Fiber in Peritoneal Fluid of Carcinomatosis

Isolated cancer cell clusters from peritoneal fluid of carcinomatosis were found to be associated with fibrin fiber. Figure 6*A* presents cell aggregates englobed by fibers that were stained with methylene blue and eosin dyes. These fibrin deposits could be observed when the clusters were examined using phase contrast microscopy (Figure 6*B*). The fibrin deposit in the cell cluster (Figure 6*C*) was also detected by immunohistochemistry analysis. Fibrin matrix in intercellular space as presented in Figure 6*D* suggests the presence of fibrin in cancer cell cluster during peritoneal metastasis. The transmission electron microscopy of cell cluster presented in (Figure 6*E*) shows the fibrin network around the cells. High magnification of fibrin reticulation presented in Figure 6*F* indicated the typical fibrin structure. These results suggest that fibrin might be helpful for the cancer cell cluster integrities.

Our *in vitro* study showed that when the cancer cells were incubated with fibrin clot generated by a pool of several human plasma (Figure 6*G*), they interacted and adhered to fibrin fiber (Figure 6*H*). The detail of phyllopod interaction with fibrin is demonstrated in Figure 6*I* (the phyllopod adhered on the fibrin net) and Figure 6*J* (the phyllopod inserted into the clot).

In parallel studies, the interaction of cancer cells with fibrin clot was analyzed by micro cinematography. Here, when the fibrin clot was incubated with culture medium, the fibrin fibers filaments disintegrated from fibrin clot body in a time dependent manner (Figure 6*M*).

In this study, we distinguished three kinds of interactions: 1) the direct interaction of cells with fibrin clot surface, 2) the interaction of the cells with detached fiber filaments that modified the kinetic of cell interaction with fibrin corpus 3) the inhibition of cells to adhere the fibrin corpus and confining the cancer cells (Figure 6*K*). The data presented in Figure 6*M* show that after 28 h of incubation of cancer cells with fibrin clot, they covered the distance 507 m length within 76 min (zone 1) while the fiber filaments generated from clots have 53 m lengths (zone 2) (the mean of 3 experiments). In this condition, the detached fiber filaments prevented the cancer cellfibrin clot interaction. Fifty minutes were taken by the cancer cells to attach the fibrin clot (speed of cell migration on the clot 0.69 to 1.05 m/min (zone 3)). Fortyfive hours later, the detached fiber filaments inhibited the interaction of cancer cells with fibrin clot body and sequestered the cancer cells. Curiously, these detached fibrins generated agglomerated cells and formed the cancer cell clusters (Figure 6*L*).

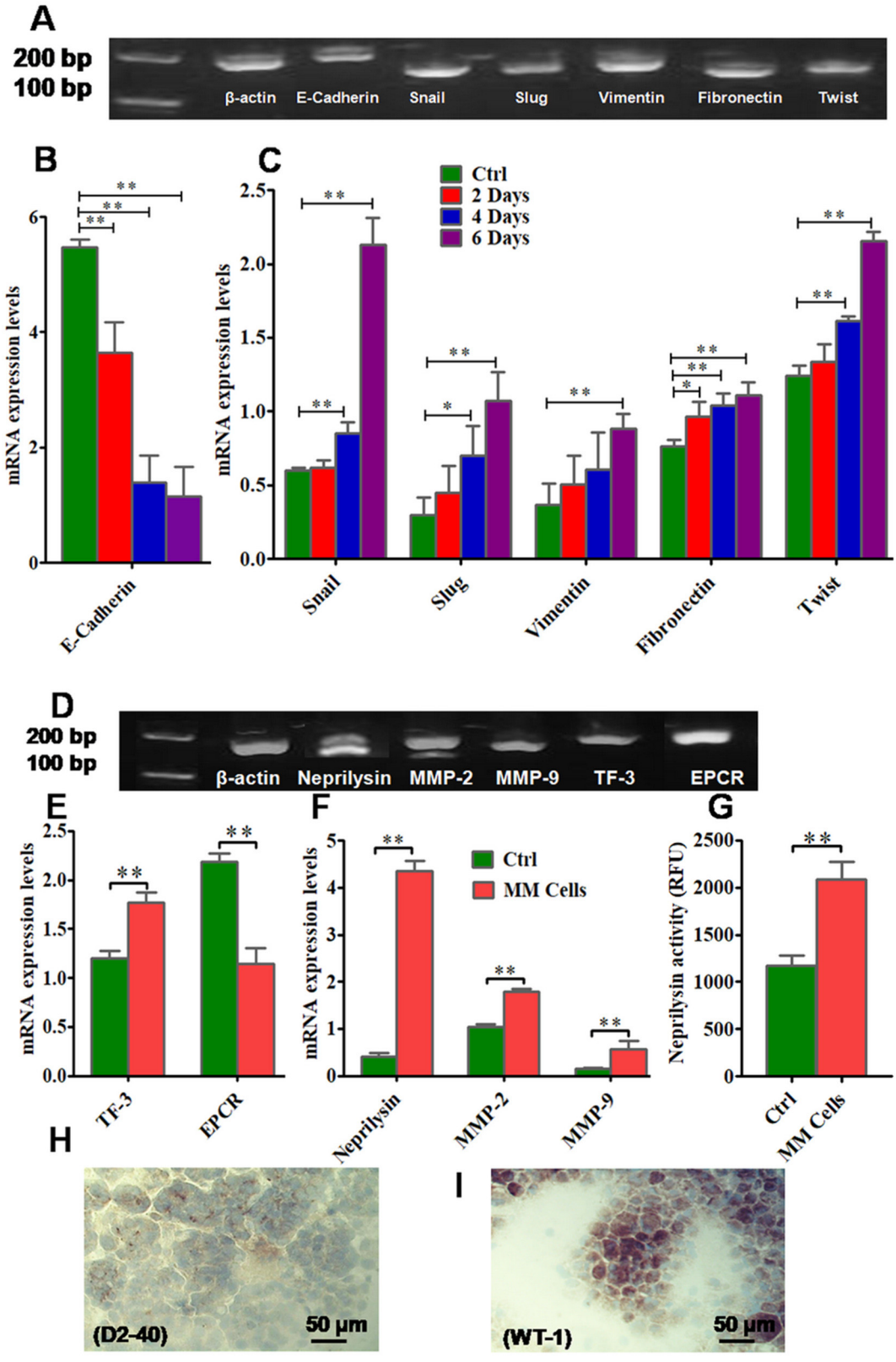

Figure 5. mRNA expression of EMT, procoagulant, anti-procoagulant and metalloprotease markers and neprilysin activity in mesothelial cells as well as immunohistochemistry of ascitic cells from ovarian cancer. mRNA of epithelial to mesenchymal transition (EMT) markers (E-cadherin, Snail, Slug, Vimentin, Fibronectin and Twist) were detected by RT-PCR (A), epithelial marker like E-cadherin was found higher (B) while mesenchymal markers (Snail, Slug, Vimentin, Fibronectin, and Twist) were found lower (D) in modified mesothelial cells (MM cells) than control (Ctrl) by qPCR; modified mesothelial cells are those treated with 25% ovarian ascites. mRNA of procoagulant (TF), anticoagulant (EPCR) and metalloprotease markers (Neprilysin, MMP-2 and MMP-9) were detected by RT-PCR (D), procoagulation marker (TF) was found higher but anti-procoagulant marker (EPCR) lower (E), metalloprotease and neprilysin were also found higher by qPCR (F) as well as neprilysin activity in modified mesothelial cells was detected higher in MM cells than ctrl (G). Protein expression level of ascitic cells is shown for Wt-1 (H) and D2–40 (I). Pictures were taken at 20 magnification. The results are expressed as mean SEM of six independent experiments. $^{*}P < .05$, $^{**}P < .01$, compared to the control (Ctrl).

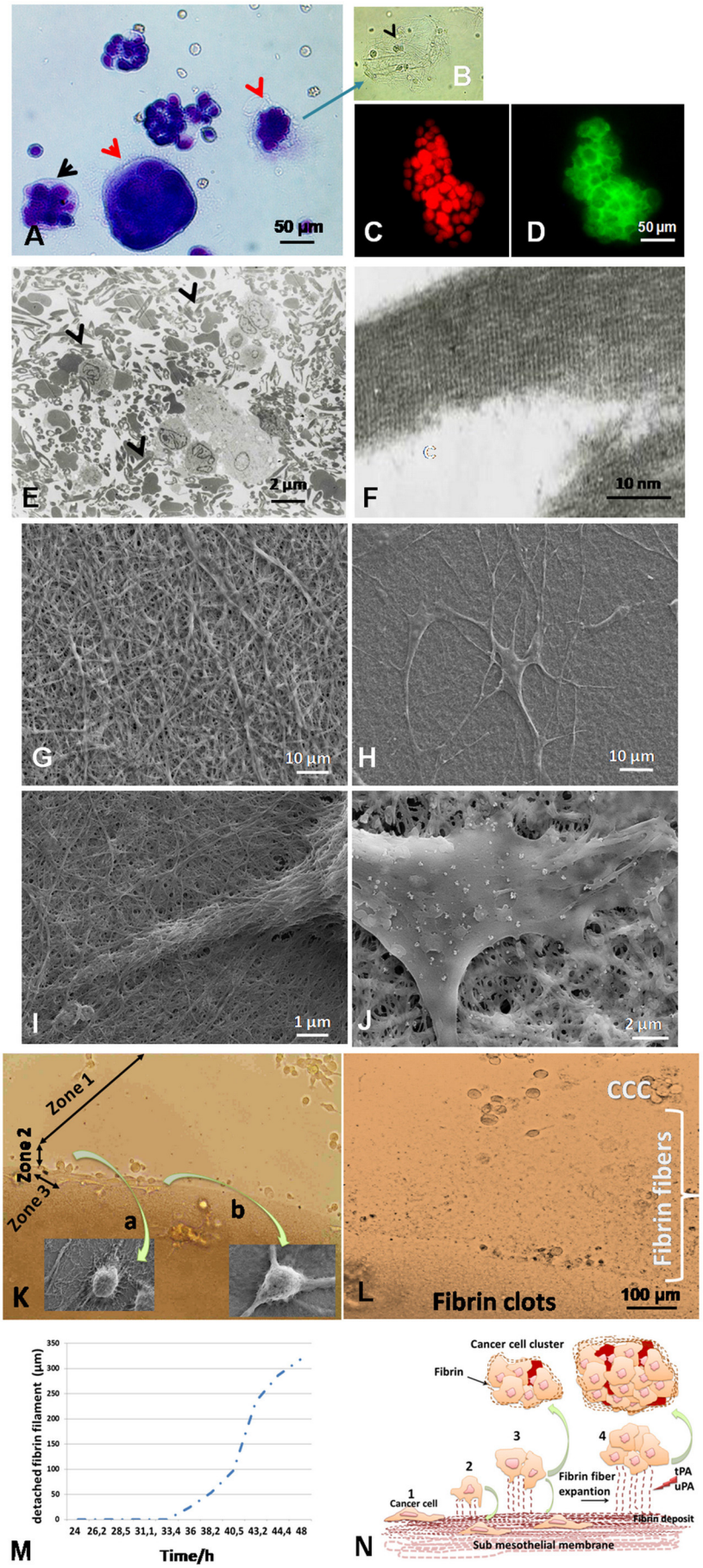
A
50 µm
B
C
D
50 µm
E
2 µm
F
10 nm
G
10 µm
H
10 µm
I
1 µm
J
2 µm
Zone 1
Zone 2
Zone 3
a
b
K
CCC
Fibrin fibers
L
Fibrin clots
100 µm
detached fibrin filament (µm)
350
300
250
200
150
100
50
0
24 26,2 28,5 31,1, 33,4 36 38,2 40,5 43,2 44,4 48
Time/h
M
Cancer cell cluster
Fibrin
1
Cancer cell
2
3
4
Fibrin fiber expantion
tPA
uPA
Fibrin deposit
Sub mesothelial membrane
N

Discussion

The natural history of peritoneal carcinoma in ovarian cancer is similar to the digestive tumor with metastasis and dissemination of peritoneum. The consequences of this phenomenon are cancer nodule formation on the peritoneal surface, ascites generation and the formation of cancer cell clusters suspended in peritoneal fluid. All these elements contribute to favorable microenvironments for the growth and dissemination of tumor cells in the peritoneal cavity.

The peritoneum, covered by mesothelial cells layer forms a nonadhesive protective surface that involves the transport of fluids as well as antigen presentation, coagulation and fibrinolysis. In the peritoneal cavity, pathologic conditions lead to peritoneal injury, mesothelial desquamation and cell migration and liberation.

In carcinomatosis, the presence of cancer cells in peritoneal cavity induces the proinflammatory state and modifies the mesothelial cell layer microenvironment [22] resulting in cell layer disruption due to change in cell polarity [23]. When mesothelial cells are cultured with the ovarian carcinomatous fluids (1 to 6 days), the cells change their shape and acquire mesenchymal characteristics as reflected by the up regulation of Slug, Snail, Vimentin, Ncadherin, Twist and Fibronectin ($P = .001$). Ecadherin, was downregulated ($P = .001$). In parallel studies by cytokine array analysis of peritoneal fluid of ovarian, colic and gastric carcinomatosis, we showed high amounts of several family of cytokines such as nerve growth factor (NGF), vascular endothelial growth, (VEGF), macrophage inflammatory proteins (MIF), immuneinflammatory, MMP/TIMP and adiponectin as well as the cytokines and growth factors involved in EMT (results not shown). These observations indicate that mesenchymal transformation of the mesothelial cells is due to favorable microenvironments, generated by carcinomatous fluids. Upregulation of fibronectin in transformed cells could be a target for cancer cell adhesion.

Carcinomatous fluids induce cancer cell migration and also considerable changes in mesothelial cytokines secretion. In conditioned supernatants of mesothelial cells, after incubation of these cells in carcinomatosis peritoneal fluid (25%), interleukin 6 (IL6), IL8, MCP1, GRO, ANG, GCP2, and hepatocyte growth factor (HGF) were upregulated. Under the same conditions, we tested the expression of some metalloproteinases such as MMP2, MMP7, MMP9 and neprilysin known as a membrane metalloendopeptidase (CD10). Among these enzymes, MMP2, MMP9 and neprilysin were upregulated significantly ($P = .001$) reflecting enhanced extracellular matrix degradation activity. The mRNA expression of neprilysin, MMP 9 and MMP 2 increased 10.4 and 1.7 times, respectively, when mesothelial cells acquired mesenchymal characteristics through EMT phenomena. This study was confirmed by neprilysin activity, examination of biopsies from ovarian carcinomatosis by immunohistochemical analysis and over expression of CD10 immunoreactivity in mesothelial cells. Curiously, all peritoneal cells extracted from ascites of ovarian or digestive cancers presented high amount of detached mesothelial cells stained with D2–40 [24] and Wilm's tumor marker (WT1) [25]. These results support the detachment of mesothelial cells in carcinomatous ascites.

When mesothelial cells were incubated with bioactive proteins (IL6, IL8, HGF, and GCP2), the upregulation of fibronectin and neprilysin as well as metalloproteases were observed. HGF and IL8 modulate the adhesion of cancer cells to the peritoneal mesothelium [26,27]. IL6 and GCP2 upregulate the tissue factor, a procoagulant protein [28]. Tissue factors were also upregulated during mesothelial mesenchymal cell transformation. Interestingly, endothelial protein C receptor (EPCR) was downregulated under the same condition [29]. The protein C as a natural anticoagulant could participate in nonclotability of carcinomatous ascites. The increased tissue factor and decreased EPCR expression on transformed mesothelial cells modified the lubrication property of mesothelial cells surface and induced procoagulant activity on the peritoneal surface. The immediate consequences of this phenomenon are fibrin formation and deposition. The presence of fibrin on the mesothelial layer of peritoneum as well as in the ascites of carcinomatous patients is in agreement with this hypothesis. Our *in vitro* studies show cancer cell adherence and penetration into the fibrin gel when incubated with the plasmatic fibrin clot. These results were confirmed by SEM and MCG analysis. The results of SEM images related to fibrin and cancer cell interaction indicate the presence of the interfibrillar pores and prolongation of cellular philopods on the gel in the fibrin network. The results were confirmed by MCG in 48 h of cancer cell fibrin gel interaction. The kinetic of cell attachment on the fibrin, in a time dependent manner, showed that attachment happened up to 7 h and gradually diminished as fibrin fibers disintegrated and were released. Interestingly, the unattached cells sequestered by the fibrin fiber in peripheral zone of fibrin clot could agglomerate and divide. In this study we measured the kinetic of fibrin fiber filaments dissociation from fibrin corpus. These results indicate that after fibrin formation on the inner peritoneal layer, the cancer cells attach to the fibrin mass and implant on the peritoneal surface. This fibrin gel in peritoneal fluid can generate the fibrin fiber and inhibit the subsequent attachment of cancer cells to the fibrin corpus. Therefore, sequestered cells could generate cancer cells clusters. The analyses of several MCG revealed that when the cancer cells attached to fibrin corpus, the cells divided and produced a cancerous nodule as shown in the supplementary video. In contrast, the sequestered cells also divided and formed the cell clusters. These clusters might be detached from peritoneal surface by fibrinolytic enzymes such as tissue plasmin activator (tPA) and urokinase (uPA) and liberated into peritoneal fluids [30]. In addition to fibrin formation, we have recently shown that these mesothelial cells have the ability to absorb sHLAG from the ascites which is an immunomodulatory protein. This absorbance of sHLAG can further aid in the attachment of cancer cells to the peritoneal surface by providing immune suppressive microenvironment [31].

In parallel studies, we observed the shape modification of mesothelial cells by SEM on the invasive and noninvasive sample from ovarian carcinomatosis patients. In the carcinomatosis zones of peritoneum, compared with noninvasive zone, the mesothelial cells presented high deformity and irregularity. Several wounds in mesothelial cell layer suggested the denudation of basal membrane of mesothelium. The morphological aspect also suggested the fibrin fiber deposition in small and vast region on the peritoneal membrane. The fibrin network having the same shape as *in vitro*, covered several zones of peritoneum on the sub mesothelial cells layer.

Figure 6. Fibrin network interaction of cancer cells. Shows cell aggregates isolated from ascites and stained with methylene blue and eosin dyes (A). Fibrin deposition with fiber filaments expansion (red arrow) and without (black arrow) was shown. The cancer cell cluster with fibrin networks (black arrow) was isolated from ascites (initial magnification of phase contrast microscopy is 40) (B). Immunohistochemical detection of fibrin deposit in cell cluster (C) and fibrin matrix in intercellular space (D) is shown. Electronic micrographs of ascitic cell clusters (650) (E), a view of fibrin fibers (71000) was analyzed by transmission electron microscopy (F). Interaction of cancer cells with the fibrin clots was analyzed by scanning electron microscopy (G-J) and photonic microscopy (K and L picture resulting from microcinematography analysis, CCC: cancer cell cluster). Graphical representation of detached fibrin filament with time was presented in (M). The diagram of different steps for cancer cell cluster formation is shown in (N), urokinase plasminogen activator (uPA) and tissues plasminogen activator (tPA).

In conclusion, the results obtained in this study indicate, for the first time, that cancerous nodules develop on the peritoneal membranes due to fibrin formation on the inner peritoneal layer, whereby the cancer cells attach to fibrin mass and implant on the membrane surface. Free fibrin fiber filaments liberated from the fibrin corpus attach to floating cancer cells which agglomerate and form globular cancer cell clusters in the ascitic fluid. These are key events in cancer cell dissemination and carcinomatosis expansion. Our finding is indeed a big stride in understanding the dilemma of peritoneal metastasis.

Supplementary data to this article can be found online at https://doi.org/10.1016/j.neo.2019.08.006.

Disclosures

The authors have no financial conflicts of interest.

Acknowledgements

We would like to thank Professor Amu Therwath for his valuable assistance.

References

1. Yung S, Chan TM. Mesothelial cells. *Peritoneal Dialysis International* 2007;**27**:S110–5.
2. Tarin D, Price JE, Kettlewell MG, Souter RG, Vass AC, Crossley B. Mechanisms of human tumor metastasis studied in patients with peritoneovenous shunts. *Cancer Research* 1984;**44**:3584–92.
3. Kenny HA, Kaur S, Coussens LM, Lengyel E. The initial steps of ovarian cancer cell metastasis are mediated by MMP-2 cleavage of vitronectin and fibronectin. *The Journal of Clinical Investigation* 2008;**118**:1367–79.
4. Casey RC, Burleson KM, Skubitz KM, Pambuccian SE, Oegema Jr TR, Ruff AP, Skubitz AP. 1-integrins regulate the formation and adhesion of ovarian carcinoma multicellular spheroids. *Am J Pathol* 2001;**159**:2071–80.
5. Burleson KM, Boente MP, Pambuccian SE, Skubitz AP. Disaggregation and invasion of ovarian carcinoma ascites spheroids. *Journal of Translational Medicine* 2006;**4**:6.
6. Iwanicki MP, Davidowitz RA, Ng MR, Besser A, Muranen T, Merritt M, Danuser G, Ince T, Brugge JS. Ovarian cancer spheroids use myosin-generated force to clear the mesothelium. *Cancer Discovery* 2011;**1**:144–57.
7. Bast Jr RC, Hennessy B, Mills GB. The biology of ovarian cancer: new opportunities for translation. *Nature Reviews Cancer* 2009;**9**:415.
8. Kenny HA, Chiang C-Y, White EA, Schryver EM, Habis M, Romero IL, Ladanyi A, Penicka CV, George J, Matlin K. Mesothelial cells promote early ovarian cancer metastasis through fibronectin secretion. *The Journal of Clinical Investigation* 2014;**124**:4614–28.
9. Witz CA, Monotoya-Rodriguez IA, Schenken RS. Whole explants of peritoneum and endometrium: a novel model of the early endometriosis lesion. *Fertility and Sterility* 1999;**71**:56–60.
10. Mutsaers SE. Mesothelial cells: their structure, function and role in serosal repair. *Respirology* 2002;**7**:171–91.
11. Cannistra SA. Cancer of the ovary. *New England Journal of Medicine* 1993;**329**:1550–9.
12. Lee J-G, Ahn J-H, Kim TJ, Lee JH, Choi J-H (2015). Mutant p53 promotes ovarian cancer cell adhesion to mesothelial cells via integrin 4 and Akt signals. *Scientific Reports* **5**, 12642.
13. Scalici JM, Arapovic S, Saks EJ, Atkins KA, Petroni G, Duska LR, Slack-Davis JK. Mesothelium expression of vascular cell adhesion molecule-1 (VCAM-1) is associated with an unfavorable prognosis in epithelial ovarian cancer (EOC). *Cancer* 2017;**123**:977–84.
14. Takatsuki H, Komatsu S, Sano R, Takada Y, Tsuji T. Adhesion of gastric carcinoma cells to peritoneum mediated by α31 integrin (VLA-3). *Cancer research* 2004;**64**:6065–70.
15. Bourboulia D, Stetler-Stevenson WG. *Matrix metalloproteinases (MMPs) and tissue inhibitors of metalloproteinases (TIMPs): Positive and negative regulators in tumor cell adhesion*, 20. Editor (ed)^(eds).City:Elsevier; 2010. p. 161–8.
16. Heino J, Ignotz RA, Hemler ME, Crouse C, Massague J. Regulation of cell adhesion receptors by transforming growth factor-beta. Concomitant regulation of integrins that share a common beta 1 subunit. *J Biol Chem* 1989;**264**:380–8.
17. Honjo K, Munakata S, Tashiro Y, Salama Y, Shimazu H, Eiamboonsert S, Dhahri D, Ichimura A, Dan T, Miyata T. Plasminogen activator inhibitor-1 regulates macrophage-dependent postoperative adhesion by enhancing EGF-HER1 signaling in mice. *FASEB Journal* 2017;**31**:2625–37.
18. Matte I, Lane D, Laplante C, Garde-Granger P, Rancourt C, Pich A. Ovarian cancer ascites enhance the migration of patient-derived peritoneal mesothelial cells via cMet pathway through HGF-dependent and-independent mechanisms. *International Journal of Cancer* 2015;**137**:289–98.
19. Bekes I, Friedl TW, Khler T, Mbus V, Janni W, Wckel A, Wulff C. Does VEGF facilitate local tumor growth and spread into the abdominal cavity by suppressing endothelial cell adhesion, thus increasing vascular peritoneal permeability followed by ascites production in ovarian cancer? *Mol Cancer* 2016;**15**:13.
20. Hofer S, Molema G, Hermens R, Wanebo H, Reichner J, Hoekstra H. The effect of surgical wounding on tumour development. *European Journal of Surgical Oncology (EJSO)* 1999;**25**:231–43.
21. Soria J, Soria C, Mirshahi M, Boucheix C, Aurengo A, Perrot J-Y, Bernadou A, Samama M, Rosenfeld C. Conformational change in fibrinogen induced by adsorption to a surface. *Journal of Colloid and Interface Science* 1985;**107**:204–8
22. Freedman RS, Deavers M, Liu J, Wang E. Peritoneal inflammation–A microenvironment for Epithelial Ovarian Cancer (EOC). *Journal of Translational Medicine* 2004;**2**:23.
23. Sandoval P, Jimnez-Heffernan JA, Rynne-Vidal , Prez-Lozano ML, Gilsanz , Ruiz-Carpio V, Reyes R, Garca-Bordas J, Stamatakis K, Dotor J. Carcinoma-associated fibroblasts derive from mesothelial cells via mesothelial-to-mesenchymal transition in peritoneal metastasis. *The Journal of Pathology* 2013;**231**:517–31.
24. Chu AY, Litzky LA, Pasha TL, Acs G, Zhang PJ. Utility of D2-40, a novel mesothelial marker, in the diagnosis of malignant mesothelioma. *Mod Pathol* 2005;**18**:105.
25. Amin KM, Litzky LA, Smythe WR, Mooney AM, Morris JM, Mews DJ, Pass HI, Kari C, Rodeck U, Rauscher III FJ (1995). Wilms' tumor 1 susceptibility (WT1) gene products are selectively expressed in malignant mesothelioma. *The American Journal of Pathology* **146**, 344.
26. Ip CK, Yung S, Chan T-M, Wong AS. Hepatocyte growth factor modulates adhesion of ovarian cancer cells to the peritoneum mesothelium through p70 S6 kinase*Editor (ed)^(eds)*.AACR:City; 2011.
27. Kuai W-X, Wang Q, Yang X-Z, Zhao Y, Yu R, Tang X-J (2012). Interleukin-8 associates with adhesion, migration, invasion and chemosensitivity of human gastric cancer cells. *World Journal of Gastroenterology: WJG* **18**, 979.
28. Chin BS, Conway DS, Chung NA, Blann AD, Gibbs CR, Lip GY. Interleukin-6, tissue factor and von Willebrand factor in acute decompensated heart failure: relationship to treatment and prognosis. *Blood Coagulation & Fibrinolysis* 2003;**14**:515–21.
29. Kerr R, Stirling D, Ludlam CA. Interleukin 6 and haemostasis. *Br J Haematol* 2001;**115**:3–12.
30. Bu L, Karlsrud T, Dyrhaug G, Bell H, Engstrom L, Johansen H, Aasen A. The fibrinolytic system in human ascites. *Scandinavian Journal of Gastroenterology* 1995;**30**:1101–7.
31. Ullah M, Azazzen D, Kaci R, Benabbou N, Lauraine EP, Pocard M, Mirshahi M. High expression of HLA-G in ovarian carcinomatosis: The role of interleukin-1. *Neoplasia* 2019;**21**:331–42.